Article

Investigation and Simulation Study on the Impact of Vegetation Cover Evolution on Watershed Soil Erosion

Dandan Shen [1], Yuangang Guo [2], Bo Qu [3,4,*], Sisi Cao [1], Yaer Wu [1], Yu Bai [1], Yiting Shao [1] and Jinglin Qian [1]

1 School of Hydraulic Engineering, Zhejiang University of Water Resources and Electric Power, Hangzhou 310018, China
2 Zhejiang Design Institute of Water Conservancy & Hydro-Electric Power Co., Ltd., Hangzhou 310016, China
3 Yellow River Institute of Hydraulic Research, YRCC, Zhengzhou 450003, China
4 Key Laboratory of Lower Yellow River Channel and Estuary Regulation, MWR, Zhengzhou 450003, China
* Correspondence: qubo_edu_hohai@163.com

Abstract: Soil erosion has always been a critical issue confronting watershed environments, impacting the progress of sustainable development. As an increasing number of countries turn their attention to this problem, numerous policies have been enacted to halt the progression of soil erosion. However, policy-driven interventions often lead to significant changes in watershed vegetation coverage, under which circumstances, the original sediment erosion models may fall short in terms of simulation accuracy. Taking the Kuye River watershed as the research subject, this study investigates soil erosion data spanning from 1981 to 2015 and utilizes the Revised Universal Soil Loss Equation (RUSLE) model to simulate soil erosion. It is found that the extensive planting of vegetation after 2000 has led to a rapid reduction in soil erosion within the Kuye River watershed. The original vegetation cover and management factor (C) proves inadequate in predicting the abrupt changes in vegetation coverage. Consequently, this study adopts two improved plant cover and management factor equations. We propose two new methods for calculating the vegetation cover and management factor, one using machine learning techniques and the other employing a segmented calculation approach. The machine learning approach utilizes the Eureqa software (version11.0, Cornell University, New York, American) to search for the relationship between Normalized Difference Vegetation Index ($NDVI$) and C, ultimately establishing an equation that describes this relationship. On the other hand, the piecewise method determines critical values based on data trends and provides separate formulas for C above and below these critical values. Both methods have achieved superior calculation accuracy. Specifically, the overall data calculation using the machine learning method achieved an determined coefficient (R^2) of 0.5959, while the segmented calculation method achieved an R^2 of 0.6649. Compared to the R^2 calculated by the traditional RULSE method, these two new methods can more accurately predict soil erosion. The findings of this study can provide valuable theoretical reference for water and soil prediction in watersheds.

Keywords: RULSE; soil erosion; vegetation cover factor; machine learning method

1. Introduction

Soil erosion is a critical factor influencing the environment of watersheds, restricting societal economic development and food security [1,2]. Soil erosion and water loss within watersheds is a complex process related to both natural and anthropogenic factors, primarily encompassing vegetation cover, land use, geological conditions, watershed characteristics, water and soil temperature, and land management practices [3,4]. The area of soil erosion in China has far exceeded 4 million square kilometers, accounting for about half of the total land area. In China, the issue of water and sediment in the Yellow River Basin has long been a focal point of scientific research, with soil erosion in this basin posing a major obstacle to the achievement of sustainable agricultural development [5,6]. The area and intensity of water and soil loss in the Yellow River basin have been somewhat

controlled over the past few decades, yet they still face severe challenges. According to publicly available information, the area and intensity of water and soil loss in the Yellow River basin have achieved a "double decline" through continuous governance. However, the Loess Plateau, which suffers from the most severe water and soil loss, still accounts for a large proportion of the total area affected in the Yellow River basin.

In recent years, an increasing number of scholars have embarked on research efforts to study soil and water loss within watersheds and analyze the main factors that influence it [7]. Numerous studies have indicated that rainfall is one of the primary factors contributing to soil erosion. Raindrops impact the soil, disrupting the particle structure and causing splash erosion of soil particles [8,9]. Vegetation has been proven to be an important part of protecting the ecological environment [10]. Vegetation, on the other hand, reduces the direct impact of raindrops on the soil due to its foliage and branches covering the soil surface, thereby mitigating soil erosion [11,12]. Therefore, improving the vegetation structure and increasing the vegetation coverage in watersheds can effectively slow down the current situation of soil and water loss. Zaimes et al. [13] studied the amount of soil erosion under four vegetation cover forms and proposed protective management measures to reduce soil erosion. To describe the influence of vegetation on soil erosion, many scholars have employed the Normalized Difference Vegetation Index (*NDVI*) as a generalized indicator of vegetation's effect on soil erosion [14]. Zaimes et al. [15] evaluated the soil erosion risk of the semi-arid Greek island of Rhodes using a combination of Analytic Hierarchy Process and Weighted Linear Combination Method based on multi criteria decision analysis.

With advancements in science and technology, the research on simulating and predicting soil erosion has become increasingly sophisticated [16,17]. The development of soil erosion models can facilitate the study of soil erosion patterns in river basins. There are various methods for simulating soil erosion, among which the commonly used ones include empirical equation methods (such as the Universal Soil Loss Equation (USLE)), physical models, and Multi-Criteria Decision Making (MCDM) techniques to identify erosion-prone areas [18]. The USLE and its derivative models, such as the Revised Universal Soil Loss Equation (RUSLE), are practical models for estimating soil loss at the watershed scale [19]. The RUSLE model is based on five primary factors of soil erosion: rainfall erosivity, soil erodibility, slope length and steepness factor, cover-management factor, and conservation practice factor. By integrating these factors, the RUSLE model can estimate the average annual soil loss. Golkarian et al. [18] combine the Frequency Ratio (FR) model with the RULSE model, aiming to determine the relationship between historical SWE (Snow Water Equivalent) data and controlling geographical and environmental factors at 116 locations within the Nowroud watershed in northern Iran. Zhou et al. [20] research was conducted in the dry-hot valley region of the Jinsha River, which is one of the major sediment-producing areas in the Yangtze River Basin. It took into account topographic factors and land cover, and applied the RUSLE combined with Geographic Information System (GIS) to quantify the contributions and variation patterns of different factors to soil erosion in the dry-hot valley. The development of these models contributes to the study of soil erosion in regional watersheds and provides theoretical references for soil and water conservation measures in these areas.

Although numerous studies have been conducted on traditional sediment erosion models, the vegetation cover coefficients established in these studies are mostly validated in areas where the vegetation cover area does not change significantly. This paper innovatively proposes two new methods for calculating the vegetation cover coefficient. Compared to the traditional, relatively modified methods for determining the vegetation cover coefficient, these new methods take into account the impact on the coefficient following drastic changes in vegetation cover area. The improved vegetation cover coefficient has a significantly broader range of applicability. With the deepening of sustainable development, China has placed increasing emphasis on the issue of soil erosion and water loss in the Yellow River Basin. Large-scale vegetation planting in this basin began after 2000, leading to significant changes in vegetation cover. Given this rapid change in vegetation cover, it remains to be

seen whether the findings of traditional models are still applicable. Taking the Kuye River Basin, a sub-basin of the Yellow River, as the research object, this paper investigates the variation patterns of rainfall, runoff, vegetation cover, and soil erosion in the Kuye River from 1981 to 2015. The study aims to explore the mechanisms that need improvement in the RUSLE under such conditions, providing a theoretical reference for predicting soil loss in similar watersheds.

2. Materials and Methods

2.1. Study Area

Kuye River, a first-order tributary of the middle reaches of the Yellow River, is situated between 38°22′ N and 39°30′ N (as illustrated in Figure 1). With a main stream length of 242 km and a drainage area of 8706 square kilometers, the Kuye River boasts a straightforward hydrological system characterized by short tributaries on both banks. There are 21 relatively significant tributaries, among which 9 are located on the northeastern bank. The Kuye River Basin suffers from severe soil erosion, leading to significant variations in both flood and dry flow rates, and thus, frequent floods. The vegetation in the Kuye River basin is sparse, with shrubs as the main vegetation in the upstream and herbaceous plants in the downstream. The watershed is severely eroded by water and wind erosion, and the proportion of soil erosion area to the total area reaches 95%.

2.2. Data Source and Processing Method

The runoff and soil erosion data used in this study were monitored by the Wenjiachuan station from 1981 to 2015, which is the hydrological control station for the Kuye river, with a catchment area of 8515 square kilometers upstream and a riverbed slope of 3.44‰. The data are primarily excerpted from hydrological yearbooks and observation records from hydrological stations provided by the Yellow River Institute of Hydraulic Research and the Bureau of Hydrology of the Yellow River Conservancy Commission. Additionally, data are extracted from publications such as the "China River Sediment Bulletin", the "Yellow River Sediment Bulletin", and the "Yellow River Water Resources Bulletin".

The *NDVI* data utilized in this research originate from a dataset provided by the Institute of Geographic Sciences and Natural Resources Research, Chinese Academy of Sciences. The data span from 1981 to 2015, with an *NDVI* data resolution of 8 km for the period 1981–1997 and 1 km for the period 1998–2015. With the implementation of policies such as the "Decision of the State Council on Soil and Water Conservation in the Middle Reaches of the Yellow River" and the "Guiding Opinions on Promoting High-Quality Development of Soil and Water Conservation in the Yellow River Basin", the vegetation coverage in the Yellow River Basin has seen a significant increase. From Table 1, it can be seen that grassland is the dominant land use type in the Kuye river basin, occupying more than half of the area in each period.

Table 1. Area proportion of different land use types in the study catchment.

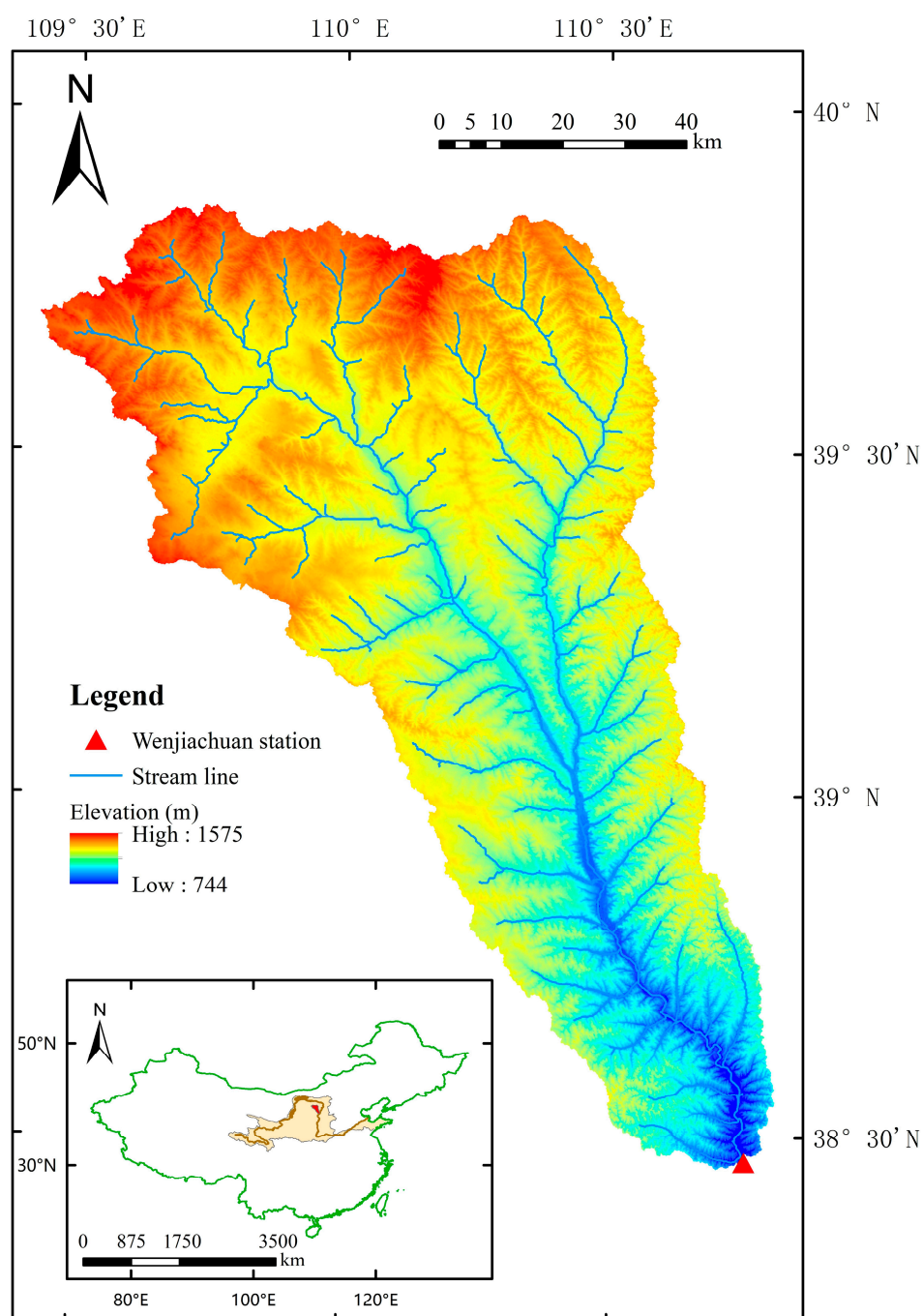|	1986	1996	2006	2011
Grass	58.6%	65.2%	52.7%	65.3%
Tree	1.5%	1.5%	7.8%	6.7%
Farmland	21%	14.2%	18.5%	11.8%
Other	18.9%	19.1%	21%	16.2%

Figure 1. The study area.

2.3. RULSE Model

The soil erosion prediction model used in this study is the widely applied RULSE model [21,22]. The RULSE model is built upon the foundation of the Universal Soil Loss Equation (USLE) originally developed in the United States [23]. It is one of the widely used soil erosion prediction models both domestically and internationally. The specific formula of the RULSE model is as follows [21]:

$$A = R \times K \times L \times S \times C \times P \tag{1}$$

where A denotes the amount of the average soil loss (t ha^{-1} year^{-1}); R represents the rainfall erosivity factor (mm ha^{-1} h^{-1} year^{-1}); K is the soil erodibility factor (t ha h ha^{-1} MJ^{-1} mm^{-1});

L and *S* respectively represent the measurements of slope steepness and slope length; *C* is the Vegetation cover and management factor; *P* indicates the conservation practice factor.

2.3.1. Slope Length (*L*) and Steepness Factor (*S*)

The slope and slope length factors in the RUSLE model were calculated in accordance with the methodologies outlined by Beskow et al. [24] and Ganasri and Ramesh [25], as follows:

$$S = \begin{cases} 10.8 sin\theta + 0.036 & \theta < 5° \\ 16.8 sin\theta - 0.5 & 5° \leq \theta < 10° \\ 21.9 sin\theta - 0.96 & \theta \geq 10° \end{cases} \tag{2}$$

$$L = (\lambda/22.13)^m, \ m = \begin{cases} 0.2 & \theta < 1° \\ 0.3 & 1° \leq \theta < 3° \\ 0.4 & 3° \leq \theta < 5° \\ 0.5 & \theta \geq 5° \end{cases} \tag{3}$$

where θ denotes the slope; λ represents the slope length; *m* is a dimensionless constant depending on the percent slope (θ).

2.3.2. Rainfall Erosivity Factor (*R*)

The average annual erosivity (*R*) equation was formulated based on the research conducted by Golkarian et al. [18]:

$$R = 0.0483(p)^{1.61} \tag{4}$$

where *p* denote the annual precipitations (mm).

2.3.3. Soil Erodibility Factor (*K*)

Soil erodibility encapsulates the extent of soil erosion attributable solely to rainfall erosivity, highlighting variations in erosion rates while other erosion factors remain constant. For the present investigation, the soil erosion factor was determined utilizing the Erosion/Productivity Impact Calculator model, which relies on soil texture as outlined by Williams [26].

$$K = (0.2 + 0.3exp(-0.0256SAN(1 - SIL)/100)) \left(\frac{SIL}{CLA + SIL}\right)^{0.3} \times \left(1.0 - \frac{0.25CA}{CA + exp(3.72 - 2.95CA)}\right) \left(1.0 - \frac{0.7SN1}{SN1 + exp(-5.51 + 22.9SN1)}\right) \times 0.1317 \tag{5}$$

where *SAN*, *SIL* and *CLA* respectively denote the sand fraction (%), silt fraction (%), and clay fraction (%); *CA* represents the soil organic carbon content (%).

2.3.4. Vegetation Cover and Management Factor (*C*)

In traditional studies, *NDVI* serves as a prevalent and effective tool for monitoring surface vegetation cover. The *C* factor in soil erosion models also ranges from 0 to +1. Consequently, many researchers have adhered to this principle to estimate the *C* factor from *NDVI*. Typically, this estimation is carried out using the following formula [27]:

$$C = exp[-\alpha\frac{NDVI}{(\beta - NDVI)}] \tag{6}$$

where, α = 1 and β = 2 [27].

2.3.5. Conservation Practice Factor (*P*)

The erosion control practice factor (*P*) represents the proportion of soil loss with implemented conservation practices compared to soil loss without any conservation measures (i.e., upslope and downslope cultivation). Its value ranges from 0 to 1, where 0 signifies an area completely free from soil erosion, and 1 represents an area with no water conservation measures in place. Land use information can effectively indicate the level of water conservation measures employed. In this study, we assume *P* = 1 for bare land, following Fang et al. [28], and *P* = 0.2 + 0.03 × slope degrees for other land types, as suggested by Wen et al. [29].

2.4. Data Analysis

For numerical models, main requirement is accuracy. In order to evaluate the accuracy of numerical model simulation, certain data analysis methods and evaluation indexes are usually used. The coefficient of determination (R^2) and mean absolute error (MAE) were adopted to evaluate the simulation performance [30]:

$$R^2 = 1 - \frac{SSE}{SST'} \tag{7}$$

$$SST = \sum_{i=1}^{N}(Y_i - meanY)^2 \tag{8}$$

$$SSE = \sum_{i=1}^{N}(Y_i - X_i)^2 \tag{9}$$

$$meanY = \frac{1}{N}\sum_{i=1}^{N}Y_i \tag{10}$$

$$MAE = \frac{\sum_{1}^{N}|Y_i - X_i|}{N} \tag{11}$$

where *N* denotes the number of lateral measuring points; *X* and *Y* represent the calculated and measured values, respectively, *SSE* is Sum of Squares for Error, *SST* is Sum of Squares for total.

3. Results

The changes in *NDVI* data are depicted in Figure 2, which reveals that *NDVI* was relatively low before 2000, generally below 0.35, and gradually increased after 2000, with a variation range of 0.292 to 0.478. The interannual variations of precipitation and runoff are shown in Figure 3. It can be observed that the variation range of precipitation is relatively small, ranging from 147 to 466 mm, whereas the variation range of runoff is significantly larger, varying between 14 and 90 mm. The interannual changes in sediment erosion are presented in Figure 4. Prior to 2000, the soil erosion rate was relatively high, reaching a maximum of 177.63 t/ha/year. However, after 2000, the sediment erosion rate dropped sharply, with the maximum decreasing to only 14.91 t/ha/year. From Table 2, it can be observed that *NDVI* exhibits a significantly positive correlation with rainfall, while displaying a significantly negative correlation with sediment erosion and runoff. Rainfall, on the other hand, shows a significant positive correlation with runoff but does not have a significant relationship with sediment erosion. Furthermore, runoff demonstrates a significant positive correlation with sediment erosion.

Table 2. The correlation between different factors.

	NDVI	**Rainfall**	**Soil erosion**	**Runoff**
NDVI	1	0.449481 **	−0.54034 **	−0.48906 **
Rainfall		1	0.247428	0.390712 *
Soil erosion			1	0.913491 **
Runoff				1

Note: * presents significance *p*-value < 0.05, ** presents significance *p*-value < 0.01.
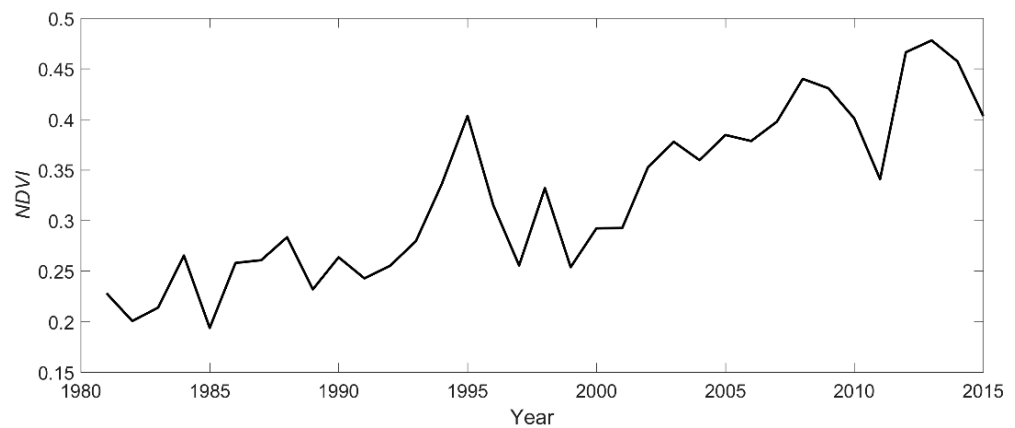
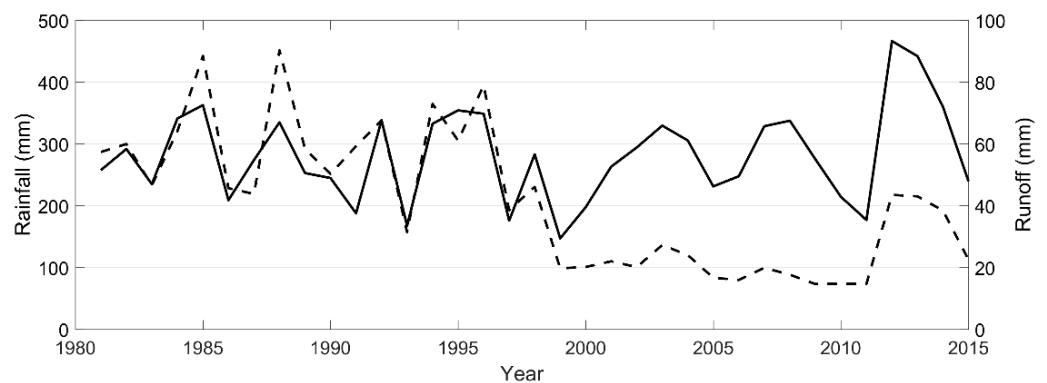**Figure 2.** The annual variation of *NDVI*.

Figure 3. The annual variation of rainfall and runoff (The solid line represents rainfall data, while the dashed line represents runoff data).
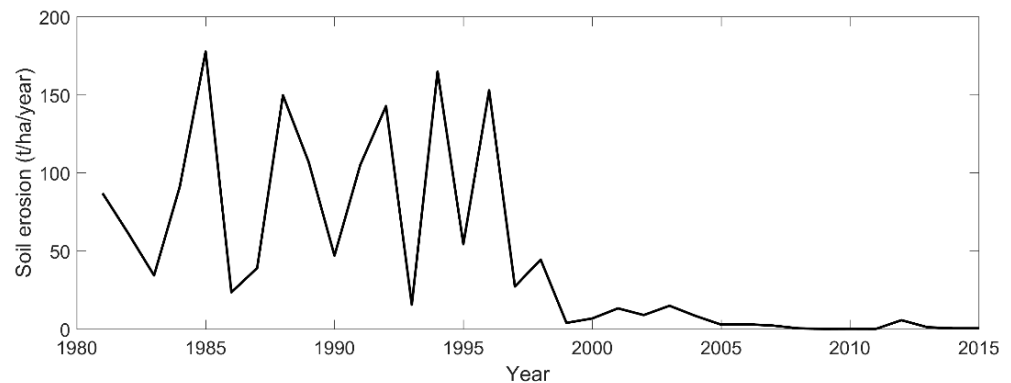

Figure 4. The annual variation of soil erosion.

Using the RULSE model, predictions of sediment erosion were made, and the results are shown in Figure 5. It can be observed that the simulation accuracy is relatively low. Most of the predicted values are higher than the measured values, which may be attributed to the sharp increase in *NDVI* values after 2000, resulting in reduced simulation accuracy of vegetation cover and management factor in Equation (6).

In this study, we propose two new methods for determining the vegetation cover and management factor. Firstly, it was hypothesized that *NVDI* and *p* are closely associated with the vegetation cover and management factor, respectively. To determine the appropriate formula form, an optimization algorithm (Eureqa) was employed in conjunction with measured data. Eureqa is an innovative computer program designed to search for numbers

in raw data and discover their correlations, thereby proposing a series of linear equations to describe these connections [30]. We establish the relationship between *NDVI*, *p*, and *C* through Eureqa and obtain the formula form for *C*.
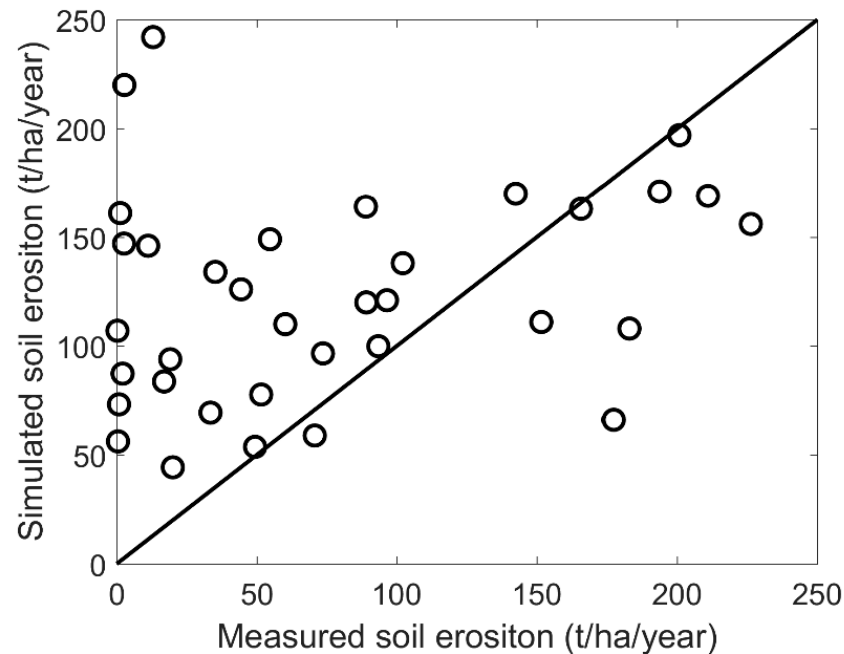
$$C = f(NVDI, p) \tag{12}$$

Figure 5. The simulation result of soil erosion by RULSE model.

Utilizing the machine learning method, Eureqa, to solve for the equation form, with 2/3 of the data used for training and 1/3 of the data used for validation, the simulation results are presented in Table 3. It can be observed that as the complexity increases, the formula form gradually becomes more intricate. Correspondingly, the accuracy of the model simulation also improves gradually (Figure 6), the formula with a complexity of 14 was selected. Then use this formula to verify the simulation effect of all data. The simulation accuracy for the training data reaches 0.7189, the accuracy for validation data is 0.3617, while the accuracy for all data is 0.5959 (Figure 7). Compared to Equation (6), the predicted values from the improved formula are more evenly distributed above and below the 1:1 line with the simulated values.

Table 3. The correlation between solution and complexity.

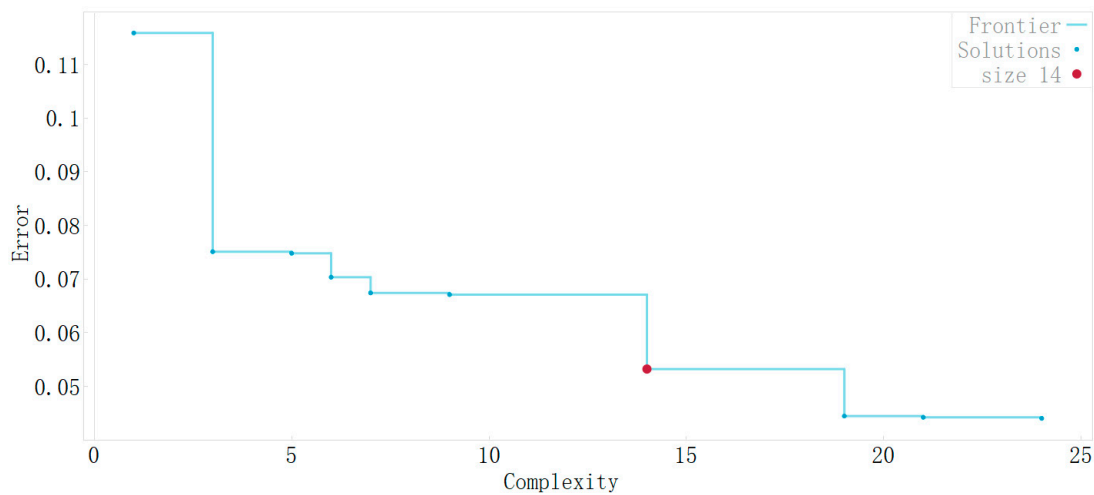| Complexity	Solution	MAE
1	$C = 0.2207$	1
3	$C = 2.47NVDI$	0.648
5	$C = 1.19 - 2.93NVDI$	0.646
6	$C = 0.25/NVDI - 0.75$	0.607
7	$C = 0.5681 + 0.0016p - 2.47NVDI$	0.582
9	$C = 0.5928 + 0.0016p - 2.5688NVDI$	0.579
14	$C = 0.5434 + 0.0018p + 0.1087\cos(p) - 2.47NVDI$	0.46
19	$C = 0.5187 + 0.0016p - 0.0395/(0.078 + \cos(0.19p)) - 2.47NVDI$	0.384
21	$C = 0.5928 + 0.0019p - 0.0395/(0.075 + \cos(0.19p)) - 2.8652NVDI$	0.382
24	$C = 0.5928 + 0.0018p - 0.0395/(0.076 + \cos(0.19p)) - 2.8899\sin(NVDI)$	0.38

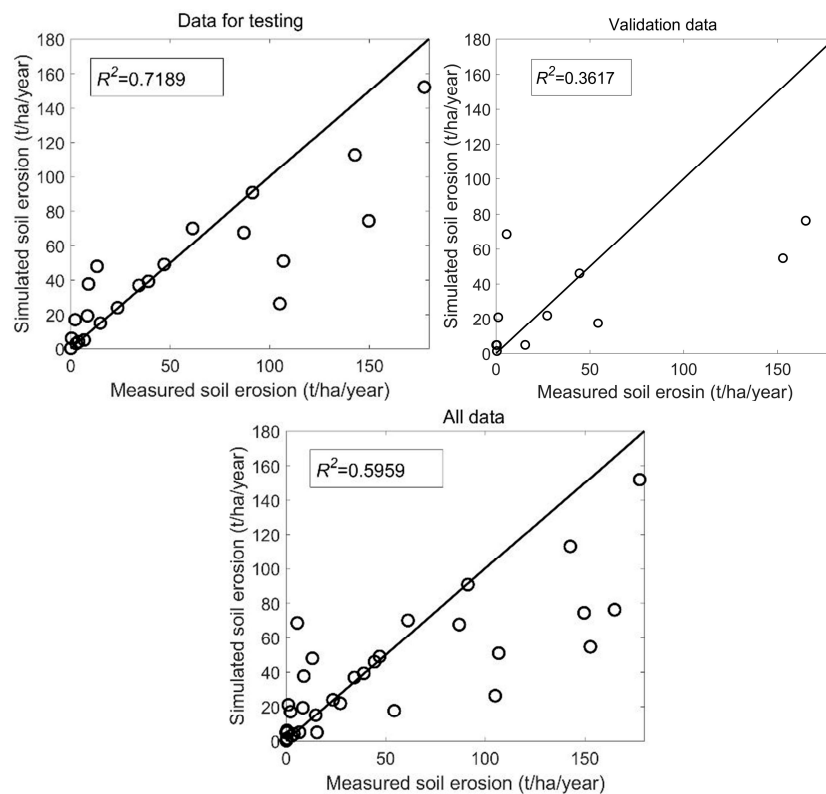**Figure 6.** The correlation between complexity and error.

Figure 7. The simulation result of soil erosion by improved RULSE model by machine learning.

The second approach involves stratifying the vegetation cover and management coefficient. The basic pattern of the model is the same as Equation (6), but the original equation is divided into two parts. Calculate *C* values greater than and less than the critical value using equations. As can be seen from the Figure 4, the year 2000 represents a significant change point in sediment erosion. Therefore, we adopt the *NDVI* data (0.3) from 2000 as the critical value, and the proposed formula form is divided into two parts as follows:

$$\begin{cases} C = \exp\left[-\alpha_1 \frac{NDVI}{(\beta_1 - NDVI)}\right] & NDVI < 0.3 \\ C = \exp\left[-\alpha_2 \frac{NDVI}{(\beta_2 - NDVI)}\right] & NDVI \geq 0.3 \end{cases} \tag{13}$$

where α_1, β_1, α_2 and β_2 are constant coefficients.

Based on 35 years of data, the constant parameters in Equation (13) were solved, resulting in the following formula. The accuracy of the simulated data is shown in Figure 8, where it can be observed that the simulated values and measured values are well distributed on both sides of the 1:1 line, with an R^2 of 0.6649, indicating a good fit between the model and the observed data.

$$\begin{cases} C = \exp\left[-3\frac{NDVI}{(2-NDVI)}\right] & NDVI < 0.3 \\ C = \exp\left[-12\frac{NDVI}{(2-NDVI)}\right] & NDVI \geq 0.3 \end{cases} \tag{14}$$
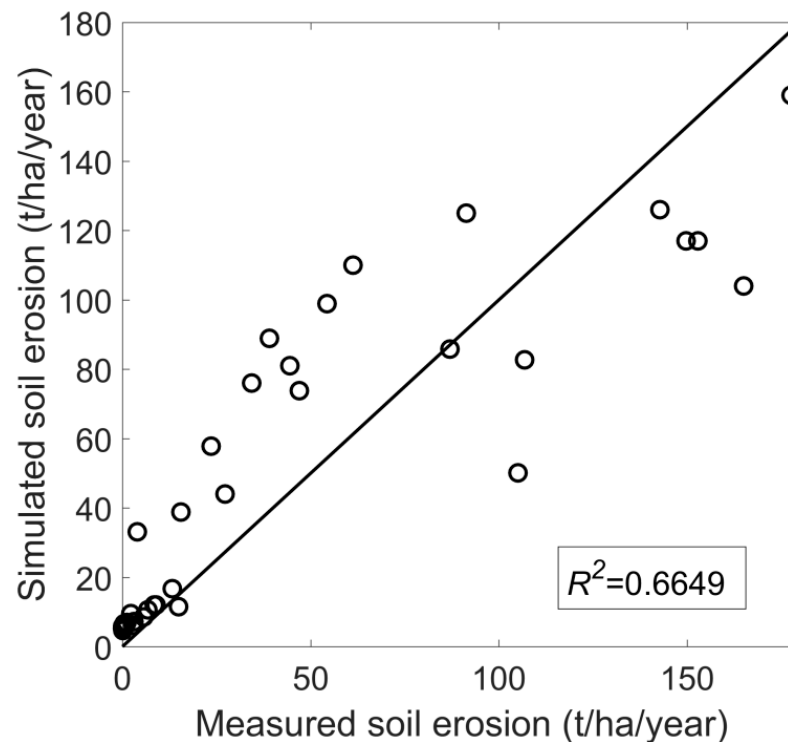
Figure 8. The simulation result of soil erosion by improved RULSE model by Equation (14).

4. Discussion

As shown in Figure 3, the runoff in Kuye river has significantly decreased since 2000, which might be related to the sudden increase of vegetation coverage. The enhanced vegetation can effectively increase the drag force on fluids during the runoff formation process, prolonging the infiltration time of runoff [31]. Furthermore, vegetation roots contribute to increasing soil porosity, thereby enhancing the infiltration rate of rainfall [32]. As shown in Table 1, there is a significant negative correlation between *NDVI*, soil erosion and runoff, the strong correlation between *NDVI*, soil erosion and runoff formation aligns with previous studies [33,34]. As shown in Table 3, the positive correlation between *NDVI* and rainfall can be attributed to several factors. One possible reason is that rainfall aids in plant growth. Research by Ratzmann et al. [35] indicates that rainfall can enhance vegetation productivity in arid and semi-arid regions, enabling them to better withstand periods of below-average rainfall. Another explanation could be the vegetation-precipitation feedback mechanism resulting from the evapotranspiration caused by vegetation, which contributes to precipitation recycling [36]. Therefore, there exists a significant positive correlation between rainfall and *NDVI*.

The data on sediment erosion, as depicted in Figure 4, reveal a significant decrease in soil erosion after 2000, which is correlated with the sharp increase in *NDVI*. Numerous studies have indicated that vegetation can effectively mitigate the splash erosion of soil by raindrops, with higher vegetation cover efficiency leading to more effective reduction

in soil loss [37]. While the RULSE model traditionally demonstrates excellent predictive performance [38], in this study, its accuracy decreases when predicting scenarios with substantial variations in *NDVI*. This discrepancy might stem from China's policies aimed at the Yellow River governance, which have resulted in a rapid and substantial increase in vegetation cover within the basin over a short period. This abrupt change in *NDVI* contrasts with previous applications of the model [39], where the original vegetation cover and management factor formulations yield relatively lower simulation accuracy under such circumstances (Figure 5). The relationship between *C* and *NDVI* based on Formula (6) is shown in Figure 9. The vegetation cover and management factor obtained from Equation (6) decreases gradually with the increase of *NDVI*, but in actual processes, the amount of soil erosion decreases slowly as *NDVI* increases. However, when *NDVI* reaches a critical value, the amount of soil erosion significantly decreases. According to the research of Chen et al. [40], it was found that when the vegetation coverage exceeds 30%, the amount of sediment erosion decreases significantly, making traditional formulas that are close to linear relationships unusable.
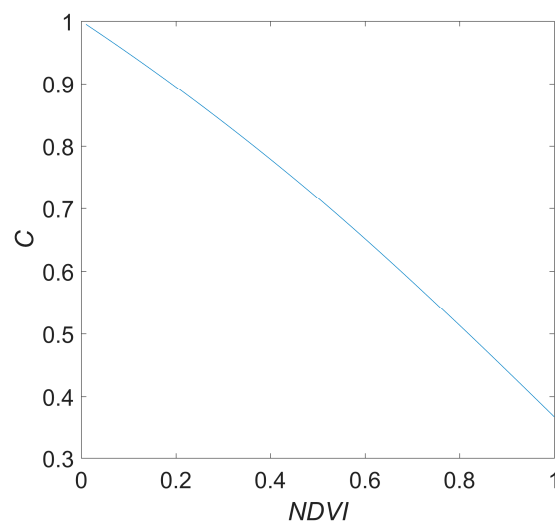

Figure 9. The relationship between *NDVI* and C by Equation (6).

At this point, it may be necessary to adopt a new formula form. Many scholars have suggested that the vegetation cover and management coefficient (*C*) is correlated with the *NDVI* and have derived equations for c based on *NDVI* [20]. As research progresses, Bai and Cui [41] found that in scenarios where *NDVI* undergoes significant temporal variations, precipitation also plays a pivotal role in influencing the vegetation coefficient. In the context of substantial variations in *NDVI*, this study incorporates the impact of precipitation on c within the formula. By employing machine learning techniques to simulate the vegetation cover and management coefficient (*C*), we have achieved promising results that account for the influence of rainfall. Alternatively, we can separately solve for the vegetation cover and management coefficient above and below the critical *NDVI* value. By comparing the two proposed new formula forms, the overall simulation effect of Equation (8) is found to be higher. This indicates that Equation (8) provides a more accurate representation of the relationship between soil erosion and *NDVI*, especially when considering the distinct behavior above and below the critical *NDVI* threshold.

As can be seen from Figure 4, a significant decline in sediment loss began around 1999. Meanwhile, Figure 2 indicates a substantial increase in *NDVI* around the same period. Therefore, we hypothesize that the average *NDVI* value (0.3) from 1998 to 2000 can be taken as the critical value. Upon testing, we found that the simulation results were satisfactory, confirming that using 0.3 as the critical value is reasonable. The first prediction method for soil and water loss is more easily generalized to other watersheds, providing a basis for soil and water loss prediction in those areas. The second method has good application

potential in watershed management, and watershed managers should strive to maintain the *NDVI* of the watershed close to the critical value to ensure minimal sediment loss.

The advancement of meteorological forecasting technology has made it possible for us to obtain future meteorological data [42], and the development of optimization algorithms has enabled people to acquire optimized management systems more swiftly [43]. The integration of precise meteorological forecasting methods, optimization algorithms, and soil erosion prediction models can better provide a basis for watershed vegetation management. As shown in Figure 10, this is our flowchart for optimizing future vegetation management systems in watersheds. Using the genetic algorithm as the optimization algorithm, vegetation management data is randomly generated into the model as optimization items, while sediment loss is incorporated into the model as the optimization function. Simultaneously, meteorological forecasting data and basic watershed parameters are input into the improved RULSE model. Then, the genetic algorithm is run, and the optimization results are output when the genetic generations are completed.
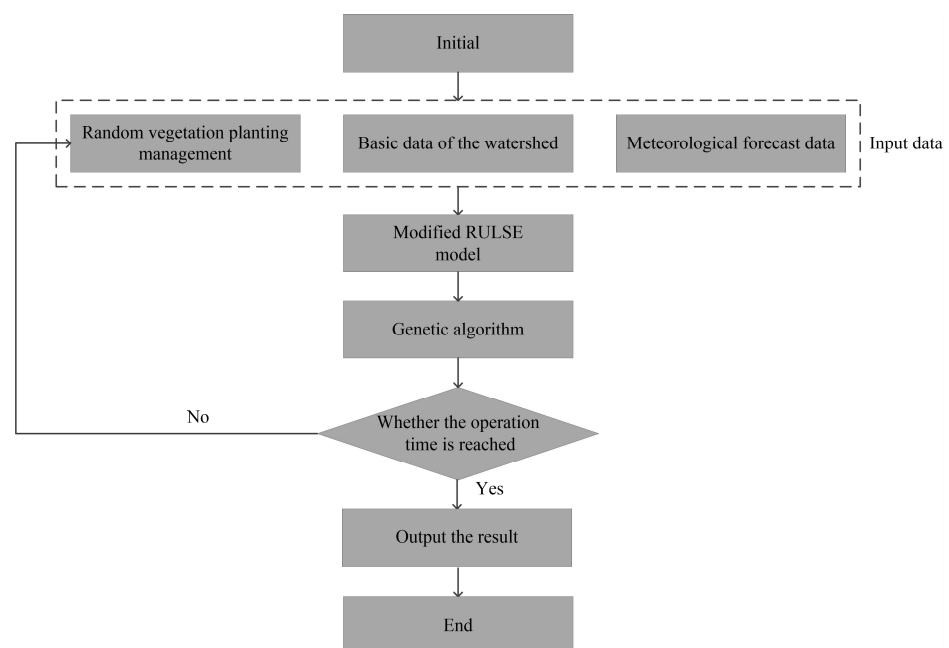

Figure 10. Schematic diagram of vegetation management measures optimization.

The current translation also has the following limitations. Firstly, the scope of validation is limited to only one watershed, and further verification across different watersheds is necessary to ascertain the model's accuracy. Secondly, despite the various improvements made to the RULSE model based on the USLE model, there are still certain limitations. For example, some parameters within the model still rely on empirical data for estimation, and the scope of application of the model is still constrained by the availability of data and the adjustment of model parameters. Therefore, in practical applications, it is necessary to validate and adjust the model in light of specific circumstances. Additionally, the model has the potential to incorporate a meteorological forecasting module, which could enable predictions of future soil erosion and water loss [44].

5. Conclusions

This study investigated the soil erosion patterns in the Kuye River using the RULSE model, yielding the following key findings:

(1) The planting of vegetation has led to a drastic reduction in both runoff and soil erosion within the Kuye River basin, demonstrating the significant role that policy guidance plays in promoting soil and water conservation efforts.

(2) The traditional formula for the vegetation cover and management factor (*C*) used in the RULSE model proved to have relatively low accuracy in simulating sediment erosion in the Kuye River basin. To address this, this study employed machine learning techniques to derive a new formula for the vegetation cover factor, which subsequently resulted in improved simulation outcomes and a more precise representation of soil erosion dynamics.

(3) Through data analysis, it was found that an *NDVI* value of 0.3 serves as a critical threshold. Applying different vegetation cover and management formulas above and below this critical value yielded better simulation results. The two proposed methods provide a theoretical reference for predicting sediment erosion in watersheds with significant variations in *NDVI*.

(4) In engineering practice, meteorological prediction methods can be combined to use the simulation method proposed in this article to predict the amount of sediment erosion in the watershed, providing reliable warnings for soil erosion. Simultaneously incorporating optimization algorithms to simulate the future sediment erosion in the watershed under different vegetation cultivation measures, and optimizing vegetation cultivation strategies.

References

1. Deng, J.; Jing, Y.; Yin, D. Soil erosion studies should consider the effect of water erosion on tillage erosion. *J. Soil Water Conserv.* **2017**, *72*, 38A–41A. [CrossRef]
2. Kuhwald, M.; Busche, F.; Saggau, P.; Duttmann, R. Is soil loss due to crop harvesting the most disregarded soil erosion process? A review of harvest erosion. *Soil Tillage Res.* **2022**, *215*, 105213. [CrossRef]
3. Yao, X.; Yu, J.; Jiang, H.; Sun, W.; Li, Z. Roles of soil erodibility, rainfall erosivity and land use in affecting soil erosion at the basin scale. *Agric. Water Manag.* **2016**, *174*, 82–92. [CrossRef]
4. Wuepper, D.; Borrelli, P.; Finger, R. Countries and the global rate of soil erosion. *Nat. Sustain.* **2020**, *3*, 51–55. [CrossRef]
5. Zhang, X.S.; Hao, F.H.; Cheng, H.G.; Li, D.F. Application of SWAT model in the upstream watershed of the Luohe River. *Chin. Geogr. Sci.* **2003**, *13*, 334–339. [CrossRef]
6. Qin, H.; Chen, F.; Liu, Y. Study on wave-influenced resistance to erosion of silty soil in Huanghe (Yellow) River Delta. *Acta Oceanol. Sin.* **2010**, *29*, 53–57. [CrossRef]
7. Zaimes, G.N.; Tamparopoulos, A.E.; Tufekcioglu, M.; Schultz, R.C. Understanding stream bank erosion and deposition in Iowa, USA: A seven year study along streams in different regions with different riparian land-uses. *J. Environ. Manag.* **2021**, *287*, 112352. [CrossRef]
8. Ohnuki, Y.; Shimizu, A. Experimental studies on rain splash erosion of forest soils after clearing in Okinawa using an artificial rainfall apparatus. *J. For. Res.* **2004**, *9*, 101–109. [CrossRef]
9. Koch, T.; Chifflard, P.; Aartsma, P.; Panten, K. A review of the characteristics of rainfall simulators in soil erosion research studies. *MethodsX* **2023**, *12*, 102506. [CrossRef]
10. Zaimes, G.N.; Gounaridis, D.; Fotakis, D. Assessing riparian land-uses/vegetation cover along the Nestos river in Greece. *Fresenius Environ. Bull.* **2011**, *20*, 3217–3225.

11. Wang, Z.J.; Jiao, J.Y.; Rayburg, S.; Wang, Q.L.; Su, Y. Soil erosion resistance of "Grain for Green" vegetation types under extreme rainfall conditions on the Loess Plateau, China. *Catena* **2016**, *141*, 109–116. [CrossRef]
12. Boukhari, Y.; Ginovart, M.; Verdú, A.M.; Mas, M.T.; Mederbal, K.; Josa, R. Hydrological soil behavior in areas with semi-arid vegetation (Beni Chougrane Mountains, Algeria). *Biologia* **2016**, *71*, 1131–1136. [CrossRef]
13. Zaimes, G.N.; Emmanouloudis, D.; Iakovoglou, V. Estimating soil erosion in Natura 2000 areas located on three semi-arid Mediterranean islands. *J. Environ. Biol.* **2012**, *33*, 277.
14. Aslam, B.; Maqsoom, A.; Alaloul, W.S.; Musarat, M.A.; Jabbar, T.; Zafar, A. Soil erosion susceptibility mapping using a GIS-based multi-criteria decision approach: Case of district Chitral, Pakistan. *Ain Shams Eng. J.* **2021**, *12*, 1637–1649. [CrossRef]
15. Zaimes, G.N.; Gounaridis, D.; Iakovoglou, V.; Emmanouloudis, D. Assessing soil erosion risk for Rhodes Island, Greece with a GIS-based multi-criteria decision analysis. In Proceedings of the IASTED International Conference on Water Resource Management, Gaborone, Botswana, 3–5 September 2012; pp. 317–324.
16. Zhang, K.; Li, S.; Peng, W.; Yu, B. Erodibility of agricultural soils on the Loess Plateau of China. *Soil Tillage Res.* **2004**, *76*, 157–165. [CrossRef]
17. Tarek, Z.; Elshewey, A.M.; Shohieb, S.M.; Elhady, A.M.; El-Attar, N.E.; Elseuofi, S.; Shams, M.Y. Soil erosion status prediction using a novel random forest model optimized by random search method. *Sustainability* **2023**, *15*, 7114. [CrossRef]
18. Golkarian, A.; Khosravi, K.; Panahi, M.; Clague, J.J. Spatial variability of soil water erosion: Comparing empirical and intelligent techniques. *Geosci. Front.* **2023**, *14*, 101456. [CrossRef]
19. Das, B.; Paul, A.; Bordoloi, R.; Tripathi, O.P.; Pandey, P.K. Soil erosion risk assessment of hilly terrain through integrated approach of RUSLE and geospatial technology: A case study of Tirap District, Arunachal Pradesh. *Model. Earth Syst. Environ.* **2018**, *4*, 373–381. [CrossRef]
20. Zhou, Y.; Yi, Y.; Liu, H.; Tang, C.; Zhang, S. Spatiotemporal dynamic of soil erosion and the key factors impact processes over semi-arid catchments in Southwest China. *Ecol. Eng.* **2024**, *201*, 107217. [CrossRef]
21. Mouris, K.; Schwindt, S.; Haun, S.; Morales Oreamuno, M.F.; Wieprecht, S. Introducing seasonal snow memory into the RUSLE. *J. Soils Sediments* **2022**, *22*, 1609–1628. [CrossRef]
22. Räsänen, T.A.; Tähtikarhu, M.; Uusi-Kämppä, J.; Piirainen, S.; Turtola, E. Evaluation of RUSLE and spatial assessment of agricultural soil erosion in Finland. *Geoderma Reg.* **2023**, *32*, e00610. [CrossRef]
23. Islam, M.R.; Jaafar, W.Z.W.; Hin, L.S.; Osman, N.; Din, M.A.M.; Zuki, F.M.; Adham, M.I. Soil erosion assessment on hillslope of GCE using RUSLE model. *J. Earth Syst. Sci.* **2018**, *127*, 50. [CrossRef]
24. Beskow, S.; Mello, C.R.; Norton, L.D.; Curi, N.; Viola, M.R.; Avanzi, J.C. Soil erosion prediction in the Grande River Basin, Brazil using distributed modeling. *Catena* **2009**, *79*, 49–59. [CrossRef]
25. Ganasri, B.P.; Ramesh, H. Assessment of soil erosion by RUSLE model using remote sensing and GIS-A case study of Nethravathi Basin. *Geosci. Front.* **2016**, *7*, 953–961. [CrossRef]
26. Williams, J.R. Chapter 25: The EPIC model. In *Computer Models of Watershed Hydrology*; Singh, V.P., Ed.; Water Resource Publication: Highlands Ranch, CO, USA, 1995; pp. 909–1000.
27. Alexakis, D.D.; Hadjimitsis, D.G.; Agapiou, A. Integrated use of remote sensing, GIS and precipitation data for the assessment of soil erosion rate in the catchment area of "Yialias" in Cyprus. *Atmos Res.* **2013**, *131*, 108–124. [CrossRef]
28. Fang, G.; Yuan, T.; Zhang, Y.; Wen, X.; Lin, R. Integrated study on soil erosion using RUSLE and GIS in Yangtze River Basin of Jiangsu Province (China). *Arab. J. Geosci.* **2019**, *12*, 173. [CrossRef]
29. Wen, X.; Deng, X.; Zhang, F. Scale effects of vegetation restoration on soil and water conservation in a semi-arid region in China: Resources conservation and sustainable management. *Resour. Conserv. Recycl.* **2019**, *151*, 104474. [CrossRef]
30. Wang, H.; Bai, Y.; Man, X.; Tang, Z.; Zhang, S. Improved RUSLE model to simulate the effect of slope forest area on soil and water conservation. *Water Supply* **2023**, *23*, 2799–2813. [CrossRef]
31. Zhang, J.; Zhang, S.; Li, G.; Liu, M.; Chen, S. Effects of vegetation lodging on overland runoff flow regime and resistance. *Water Supply* **2020**, *20*, 1463–1473. [CrossRef]
32. Dunne, T.; Zhang, W.; Aubry, B.F. Effects of rainfall, vegetation, and microtopography on infiltration and runoff. *Water Resour. Res.* **1991**, *27*, 2271–2285. [CrossRef]
33. Kim, H.W.; Kim, J.H.; Li, W.; Yang, P.; Cao, Y. Exploring the impact of green space health on runoff reduction using NDVI. *Urban For. Urban Green.* **2017**, *28*, 81–87. [CrossRef]
34. Yue, S.; Huang, J.; Zhang, Y.; Chen, W.; Guo, Y.; Cheng, M.; Ji, G. Quantitative evaluation of the impact of vegetation restoration and climate variation on runoff attenuation in the Luan River Basin based on the extended Budyko Model. *Land* **2023**, *12*, 1626. [CrossRef]
35. Ratzmann, G.; Gangkofner, U.; Tietjen, B.; Fensholt, R. Dryland vegetation functional response to altered rainfall amounts and variability derived from satellite time series data. *Remote Sens.* **2016**, *8*, 1026. [CrossRef]
36. Zhou, J.; Jia, L.; Menenti, M.; van Hoek, M.; Lu, J.; Zheng, C.; Yuan, X. Characterizing vegetation response to rainfall at multiple temporal scales in the Sahel-Sudano-Guinean region using transfer function analysis. *Remote Sens. Environ.* **2021**, *252*, 112108. [CrossRef]
37. Jomaa, S.; Barry, D.A.; Brovelli, A.; Heng, B.C.P.; Sander, G.C.; Parlange, J.Y.; Rose, C.W. Rain splash soil erosion estimation in the presence of rock fragments. *Catena* **2012**, *92*, 38–48. [CrossRef]

38. Cheng, Q.; Cai, Q.; Ma, W. Comparative study on rain splash erosion of representative soils in China. *Chin. Geogr. Sci.* **2008**, *18*, 155–161. [CrossRef]
39. Kumar, N.; Singh, S.K. Soil erosion assessment using earth observation data in a trans-boundary river basin. *Nat. Hazards* **2021**, *107*, 1–34. [CrossRef]
40. Chen, J.; Xiao, H.; Li, Z.; Liu, C.; Wang, D.; Wang, L.; Tang, C. Threshold effects of vegetation coverage on soil erosion control in small watersheds of the red soil hilly region in China. *Ecol. Eng.* **2019**, *132*, 109–114. [CrossRef]
41. Bai, Y.; Cui, H. An improved vegetation cover and management factor for RUSLE model in prediction of soil erosion. *Environ. Sci. Pollut. Res.* **2021**, *28*, 21132–21144. [CrossRef]
42. Pérez-Vega, A.; Travieso-González, C.M.; Hernández-Travieso, J.G. An approach for multiparameter meteorological forecasts. *Appl. Sci.* **2018**, *8*, 2292. [CrossRef]
43. Burks, A.R.; Punch, W.F. An analysis of the genetic marker diversity algorithm for genetic programming. *Genet. Program. Evolvable Mach.* **2017**, *18*, 213–245. [CrossRef]
44. Rao, W.; Shen, Z.; Duan, X. Spatiotemporal patterns and drivers of soil erosion in Yunnan, Southwest China: RULSE assessments for recent 30 years and future predictions based on CMIP6. *Catena* **2023**, *220*, 106703. [CrossRef]